MATERIALS RESEARCH LETTERS

Mater. Res. Lett., 2013
Vol. 1, No. 3, 161–167, http://dx.doi.org/10.1080/21663831.2013.804218

Taylor & Francis
Taylor & Francis Group

www.tandfonline.com/toc/tmrl20/current

Stabilization of bcc Mg in Thin Films at Ambient Pressure: Experimental Evidence and *ab initio* Calculations

A. Junkaew[a*], B. Ham[b], X. Zhang[a,b], A. Talapatra[b] and R. Arróyave[a,b]

[a]*Department of Materials Science and Engineering, Texas A&M University, College Station, TX 77843, USA;*
[b]*Department of Mechanical Engineering, Texas A&M University, College Station, TX 77843, USA*

(*Received 18 March 2013; final form 6 May 2013*)

Recent experiments suggest that bcc Mg can be stabilized when grown together with bcc Nb in Mg/Nb multilayer films at ambient conditions. This finding is remarkable as (pure) bcc Mg has only been observed under very high pressures and is in fact (mechanically) unstable under room conditions. Density functional theory calculations were performed to gain insight into the stability of Mg in the bcc structure. Calculations of the thermodynamic, electronic and structural stability of bcc Mg show that this structure is in fact metastable under thin film conditions, when Mg grows epitaxially on bcc Nb, in agreement with experiments.

Keywords: bcc Mg, Mg/Nb Multilayer Thin Films, Metastable Structure, Burger's Path, DFT Calculations

Introduction Magnesium (Mg) is one of the most attractive metals for the aerospace and automotive industries due to its high specific strength.[1] Under ambient conditions, bulk Mg exists in the hexagonal close packed (hcp) crystal structure, which has limited ductility due to the reduced number of active slip systems at room temperature.[1] In bulk systems, alloying with cubic elements can be used to stabilize Mg-based cubic solid solutions. Unfortunately, Mg either forms miscibility gaps or numerous intermetallic compounds when alloyed with cubic elements. A notable exception is the Mg–Li system, in which an fcc solid solution is stabilized with only 30 at.% Li.[1–3]

Under non-bulk thermodynamic constraints (i.e. in thin film or nano-structures), phase stability can be modified through the introduction of coherency constraints [4] and it is likely that Mg-based solid solutions with a wider range of alloying elements can be stabilized. Recent work aimed at improving the limited [5] hydrogen storage properties of Mg-based systems by Tan et al. [6] has shown that it is possible to stabilize a bcc Mg-based solid solution with the addition of 25 at.% Nb in co-sputtered thin films. Although theoretical and experimental work shows that Mg can be stabilized in fcc and bcc structures (under bulk and thin-film conditions) through alloying, pure Mg in the bcc structure has only been stabilized at extremely high pressures (~50 GPa) in the work reported by Olijnyk and Holzapfel.[7] In fact, bcc Mg turns out to be dynamically unstable under normal conditions, as will be discussed below. The phase diagram and phase transformation of Mg have been investigated by others,[8,9] but these studies have been limited to the stable bulk phases.

Recently, Ham et al. showed that bcc Mg can be stabilized in Mg/Nb multilayers [10] under ambient conditions. These results [10] *may constitute the first instance of experimental evidence showing that it is possible to stabilize pure bcc Mg under ambient temperature/pressure conditions*. The present authors have also demonstrated that Mg/Nb multilayers with a thickness of a few nanometers have a much higher mechanical strength compared to bulk Mg [10] and much better hydrogenation performance compared to bulk Mg.[11]

As an example, a high resolution transmission electron microscopy (HRTEM) image of the interface in Mg/Nb 5 nm multilayer in Figure 1(a) shows an occurrence of bcc Mg in the region close to the interface along with Nb. The bcc Mg grows epitaxially on top of Nb, as confirmed by the fast Fourier transform (FFT) of the high resolution image in Figure 1(b). The X-ray diffraction (XRD) pattern in Figure 1(c) shows the major peak

*Corresponding author. Email: janchalee@neo.tamu.edu

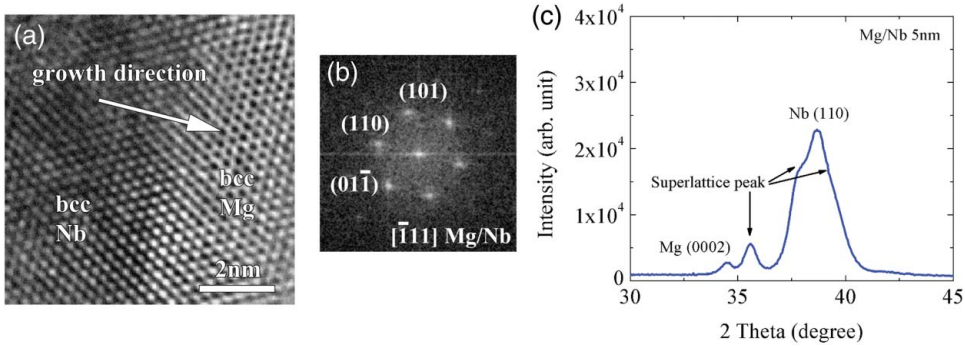

Figure 1. (a) HRTEM micrograph of Mg/Nb 5 nm multilayers showing the interface between Mg and Nb. Mg with bcc phase has grown epitaxially on Nb. (b) The FFT of Mg and Nb confirms the epitaxial relation between bcc Mg and Nb. (c) The XRD pattern of the specimen.

at the Nb(110) position. Superlattice peaks are observed on the shoulder of the Nb peak. The signal for hcp–Mg (0002) is weak and overlaps with a satellite peak due to the formation of bcc Mg near the Nb layer interface.

Stimulated by this experimental observation, this paper attempts to further elucidate the apparent (meta)stability of bcc Mg through *ab initio* calculations at 0K. While the paper focuses exclusively on the particular case of epitaxially grown Mg/Nb multilayers, this research can provide more general insight into the stabilization of bcc Mg in nano-structured alloy systems.

Results and Discussions In this work, we used electronic structure calculations based on the density functional theory (DFT) as implemented in the Vienna *ab initio* simulation package (VASP).[12,13] For more details on the specific methods and parameters of the calculations, please refer to the Supplementary Materials section.

The optimization of three structures—hcp Mg, bcc Mg and bcc Nb—was performed by *ab initio* calculations. In the case of bcc Mg, there are two initial structures constructed using a bcc structure: one using Nb's lattice parameter and another (bcc) structure with a lattice parameter corresponding to that of bcc Mg observed at very high pressures by Olijnyk and Holzapfel.[7] The full relaxations were done by optimizing all the ion positions, volume and shape of the cells. In the case of bcc Mg, in addition to full relaxations, we also performed calculations in which the lattice parameters (volumes and shapes) were constrained in order to simulate bcc Mg grown epitaxially on bcc Nb as well as high pressure bcc Mg.

Thermodynamic Stability. The optimized structural parameters and formation enthalpies of the structures mentioned above are reported in Table 1. The formation enthalpy ΔH was calculated by using the element in the gas phase as the reference state. The calculated ΔH of hcp Mg is higher than the experimental value by about 2%. Moreover, the stability of simulated Mg crystals can be evaluated by comparing their ΔH values. In hcp Mg, the calculated lattice constants show good agreement with previous work.[14] ΔH of hcp Mg is lower (more negative) than both types of bcc Mg. This implies that Mg is more stable in the hcp phase. The simulation shows that if relaxation is allowed, both types of constrained bcc Mg (grown epitaxially on bcc Nb with $a = 3.324$ Å and pressurized bulk with $a = 2.953$ Å) will relax to a lattice parameter of 3.571 Å. On the other hand, bcc Mg relaxes to an atomic volume similar to that calculated for hcp Mg ($\sim$23 Å^3). This relaxed structure corresponds to the (unstable) equilibrium bcc Mg structure at 0 K.

Lattice Dynamics. Further investigation of the effects of the lattice parameter on the stabilization of bcc Mg was done by examining the lattice dynamical properties of bcc Mg at multiple lattice parameters. The phonon dispersion relations in the bcc Mg phase were investigated by using the direct force constant method. Three forms of bcc Mg were considered: fully relaxed bcc Mg ($a = 3.571$ Å), bcc Mg with the lattice parameter of bcc Nb ($a = 3.324$ Å) and bcc Mg under high pressure with a lattice parameter of 2.953 Å.[7] Figure 2(a) shows the phonon dispersion relations along selected symmetry directions $N[\frac{1}{2}, 0, 0] \rightarrow \Gamma[0, 0, 0] \rightarrow H[\frac{1}{2}, \frac{1}{2}, -\frac{1}{2}] \rightarrow P[\frac{1}{4}, \frac{1}{4}, \frac{1}{4}] \rightarrow \Gamma[0, 0, 0]$ for the three bcc structures. Since the primitive cell of bcc Mg consists of a single atom, there are only acoustic branches in the dispersion curve.

The figure clearly shows that the fully relaxed bcc Mg structure shows negative (imaginary) frequencies along the $\Gamma - N$ direction in the Brillouin zone. This instability in the phonon structure indicates that this crystal is actually mechanically unstable: any distortion along the directions corresponding to the unstable (imaginary) phonon modes results in a spontaneous transformation to a dynamically stable state of lower energy (hcp, for example). Remarkably, Figure 2(a) shows that these unstable

Table 1. Formation enthalpies (ΔH) and calculated lattice parameters of hcp Mg, bcc Mg and bcc Nb.

Structure	ΔH (kJ/mol)	Lattice parameter (Å)	
		Calculation	References
hcp Mg			
Full relaxation	−142.6 (−145.90 ± 0.80) [15]	$a = 3.198$ ($c/a = 1.621$)	$a = 3.22$ ($c/a = 1.624$) [16]
bcc Mg			
Full relaxation	−139.7	$a = 3.571$	$a = 3.571$ [17]
Constraint (at high pressure lattice parameter)[a]	−22.2	$a = 2.953$	$a = 2.9530 \pm 0.002$ [7]
Constraint (lattice coherency with bcc Nb)[b]	−126.1	$a = 3.324$	
bcc Nb			
Full relaxation	−677.0	$a = 3.324$	$a = 3.300$ [18]

[a]Lattice parameter corresponds to the experimental lattice parameter determined experimentally at 50 GPa.[7]
[b]bcc Mg with $a = 3.324$ Å was observed experimentally as Mg grew epitaxially on Nb.

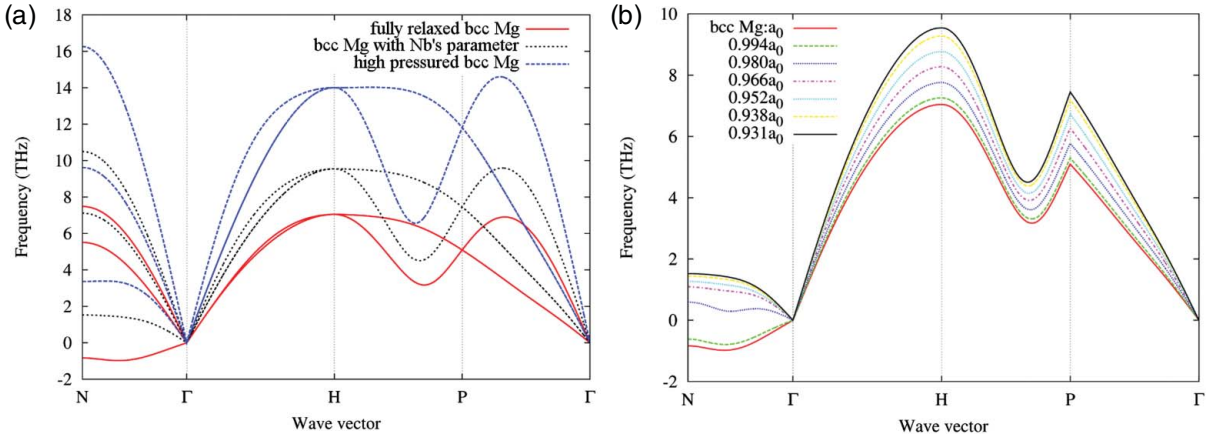

Figure 2. Phonon dispersion curves along the symmetry directions (a) comparison of calculated phonon dispersion relations of fully relaxed bcc Mg, bcc Mg with bcc Nb's lattice parameter and high-pressured bcc Mg (b) comparison of acoustic branches of varied lattice parameters (frequency in THz versus wave vector in arbitrary units).

modes are not observed in the constrained bcc Mg with a lattice parameter corresponding to bcc Nb. The phonon branches are even harder (higher frequencies) for the bcc Mg structure corresponding to high pressure experiments. This indicates that the softening of the transverse acoustic (TA) branch tends to disappear as the lattice parameter of the structure decreases. This hardening of the phonon branches is consistent with the observed stabilization of bcc Mg in regions close to the Mg/Nb interfaces.

We also notice that even though ΔH of both types of constrained bcc Mg is greater than that of fully-relaxed bcc Mg, the (compressed) metastable structures can be stabilized under the following specific conditions: either high hydrostatic pressure or constraints arising from interfacial interactions between Nb and Mg. In fact, interfacial and other thermodynamic effects, which are important in nano-scale systems, can promote the stabilization of metastable phases in thin films.[4,19,20]

Further insight into the stabilization of bcc Mg can be derived by studying the evolution of the phonon dispersion with lattice parameter, varying from that corresponding to the fully relaxed bcc Mg 3.571 Å (a_0, $V_0 = 22.769$ Å^3/atom) to bcc Mg with the lattice parameter of Nb 3.324 Å ($0.931a_0$, $V = 18.363$ Å^3/atom). The phonon dispersion curves of bcc Mg with varied lattice constants were calculated using the PHONON code. The gradual dynamic stabilization of bcc Mg can be observed as the lattice constant deceases. In fact, Figure 2(b) shows that the unstable TA mode vanishes with a decrease of 2–3.4% in the lattice parameter. The appearance of these soft modes agrees well with previous work.[21] The softening of the TA mode along the $\Gamma - N$ direction, represented by $[\xi, \xi, 0]$, indicates an instability along $[1\bar{1}0]$ planes. The softening of this phonon branch has been deemed responsible for structural transformations of bcc metals.[22,23] Here we would like to note that the calculated tetragonal shear constant $C' = (C_{11} - C_{12})/2$ for the fully relaxed bcc Mg structure is very close to zero (∼2 GPa), very close to the Born stability limit [24] (see Supplementary Materials section).

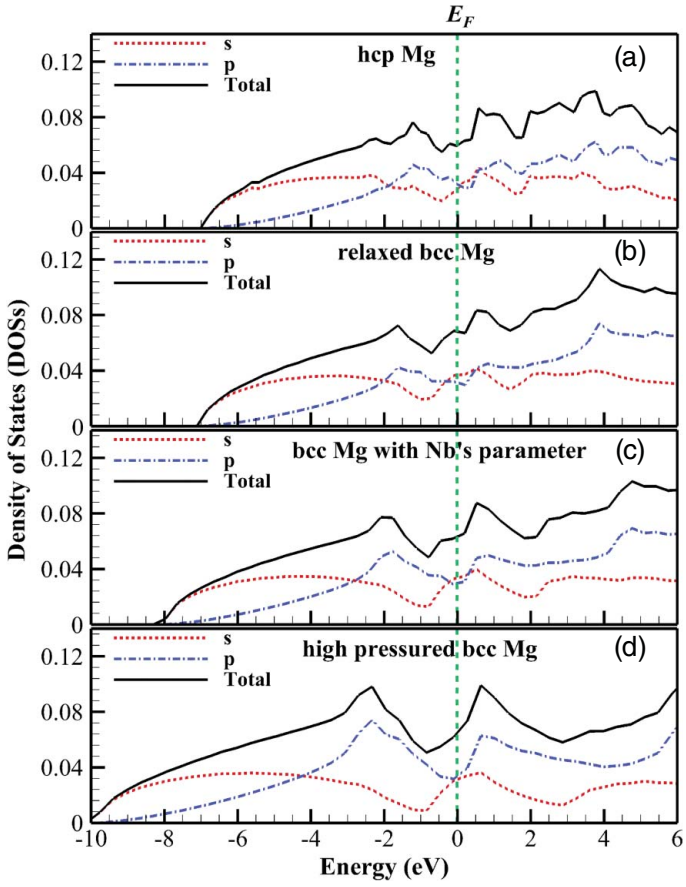

Figure 3. Partial density of states (DOS) in (a) hcp Mg, (b) relaxed bcc Mg, (c) bcc Mg with bcc Nb's lattice parameter and (d) high-pressured bcc Mg. Fermi level (E_F) is represented by an vertical dashed line.

Electronic Density of States (DOS). In this section, the electronic structure of Mg crystals is studied by analyzing the electronic Density of States (e-DOS). Total and partial e-DOS plots of hcp Mg, relaxed bcc Mg, bcc Mg with bcc Nb's lattice parameter and bcc Mg under high pressure are presented in Figure 3(a)–(d), respectively. The figure shows that all structures exhibit metallic-type bonding with occupied states at the Fermi level. For the hcp Mg crystal, the calculated e-DOS is in agreement with previous studies.[25,26] DOS plots of bcc Mg with decreasing cell volume are shown in Figure 3(b)–(d), respectively. Smaller bcc unit cell leads to a shifting of the Fermi energy level (E_F) to higher energies and qualitatively changes in the e-DOS close to E_F. In the fully relaxed bcc Mg, the local maximum of the e-DOS at the Fermi level, which is an indication of instability, is observed in Figure 3(b). Our calculations suggest that this local maximum/instability no longer appears as the volume decreases. Decreasing the volume of the bcc Mg cell also leads to a reduction in the number of electronic states (at E_F). These changes are also correlated to a larger partial e-DOS in the p-channels at the expense of the s-states at energies close to E_F. In fact, close inspection of Figure 3 suggests that s-states in a bcc-like environment make the structure unstable and it is the slight dominance—most evident at the smallest lattice parameter considered—of p-states with decreased volume which stabilizes the bcc structure. The (slight) predominance of *p*-states at E_F can also be observed in fully relaxed hcp Mg (Figure 3(a)). Moriarty et al. suggested that decreasing the atomic distance in compressed bcc Mg can result in lowering and partial filling of empty 3d bands, which in the end results in stronger interatomic bonds and a more stable structure.[27]

Burgers' Transformation. The transformation path proposed by Burgers when studying the bcc-hcp transformation in Zirconium (Zr) [28] has been used to describe the bcc-hcp transition in many metals such as barium (Ba),[29] titanium (Ti),[30] and iron (Fe).[31] The crystallographic orientation relations during the bcc-hcp transition are typically $(110)_{bcc}||(0001)_{hcp}$ and $[110]_{bcc}||[11\bar{2}0]_{hcp}$.[28] This transition consists of shearing and shuffling in specific directions and planes.

The simplest bcc to hcp transition occurs through the (intermediate) base-centered orthorhombic structure (oS4) by keeping the atomic volume constant. Two independent processes are necessary to realize this transformation: first, a shear deformation from bcc (110)

planes to the hexagonal basal plane and, second, an alternate shuffle along the $[1\bar{1}0]$ direction of the planes. The deformation during the Burgers transformation is quantified in terms of two order parameters denoted as λ_1 and λ_2, which represent shear deformation and shuffle displacement, respectively. By starting with the bcc lattice parameter a, the intermediate orthorhombic lattice parameters vary during the transition according to the following relations:

$$a_0(\lambda_1) = \frac{a}{\alpha(\lambda_1)}, \quad b_0(\lambda_1) = \alpha(\lambda_1)\sqrt{2}a, \quad c_0 = \sqrt{2}a, \tag{1}$$

where

$$\alpha(\lambda_1) = 1 + \left[\left(\frac{3}{2}\right)^{\frac{1}{4}} - 1\right]\lambda_1,$$
$$\alpha = \left[\left(\frac{1}{\sqrt{2}}\right)\tan\left(\frac{\theta}{2}\right)\right]^{1/2} \tag{2}$$

In the bcc and hcp structures, θ takes values of 109.47° and 120°, respectively. The positions of the two atoms in the cell, x_1 and x_2 are given by $[(3+\lambda_2), (3+\lambda_2)/12, 1/4]$ and $[-(3+\lambda_2, -(3+\lambda_2)/12, -1/4]$, respectively. (λ_1, λ_2) is (0,0) for the bcc structure, and (1,1) for the hcp structure, respectively.

Figure 4(a) and 4(b) show the calculated total energy contours as a function of (λ_1, λ_2) in relaxed bcc-Mg and bcc-Mg with bcc-Nb's lattice parameter, respectively. The Burgers path shown in Figure 4(a) corresponds to the transformation from fully relaxed bcc Mg($a =$ 3.571 Å, $V = 45.538$ Å^3/f.u.) to hcp Mg($a = 3.227$ Å, $c = 5.050$ Å, $c/a = 1.565$). For the case of bcc Mg with Nb's lattice parameter, the initial bcc structure with $a = 3.324$ Å ($V = 36.727$ Å^3/f.u.) is transformed to the hcp Mg ($a = 3.004$ Å, $c = 4.701$ Å, $c/a = 1.565$) shown in Figure 4(b). In both contours, the bcc structures are located at unstable/metastable saddle points, while the hcp structures are located at the global minima. This result is reasonable as the hcp Mg is more stable than the bcc Mg structure in a bulk form.

The minimum energy path (MEP) was analyzed in both systems. The MEP for the Burgers transformation is identified by using the modified string method proposed by Weinan et al. [32] which is derived from the zero temperature string method.[33] From the MEP analysis, energy barriers as a function of λ_1 and λ_2 of both models are compared in Figure 4(c). The lines with red circle and black square markers represent the MEP of fully relaxed bcc Mg and bcc Mg with Nb's parameter, respectively. The magnitude of the energy difference between fully relaxed bcc Mg (0,0) and hcp Mg (1,1) is 2.566 kJ/mol, while the magnitude of the energy difference between bcc Mg with Nb's lattice parameter and hcp Mg is 1.817 kJ/mol. Moreover, it can be observed that the bcc structure corresponding to the Burgers transformation of bcc Mg with the lattice parameter of bcc Nb actually sits on a metastable saddle point along the energy landscape. This means that the transformation from bcc to hcp Mg is not spontaneous as there is a finite (albeit small) energy barrier to the transformation. This is not the case for bcc Mg with a fully relaxed lattice parameter. In this latter case, the bcc-hcp transformation is barrier-less, and therefore spontaneous.

Interface Calculations. In addition to the foregoing analysis, the stability of Mg/Nb thin films in which bcc Mg thin films are assumed to grow epitaxially on a much thicker bcc Nb substrate were calculated using DFT methods. In these calculations, we considered two different configurations: bcc Mg/bcc Nb and coherent (pseudo)hcp Mg/bcc Nb. 10 monolayers of Nb and 4 monolayers of Mg were used. An additional vacuum

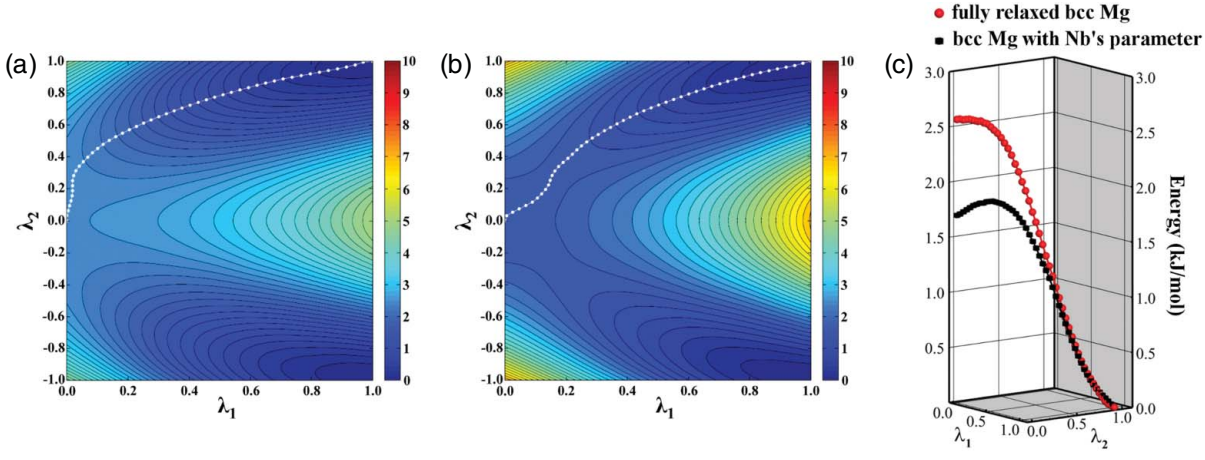

Figure 4. The total energy contour (kJ/mol) as a function of λ_1 and λ_2 for the Burgers' paths of (a) fully relaxed bcc Mg and (b) bcc Mg with bcc Nb's lattice parameter. Minimum energy path (MEP) is represented by white dots. The contour step is 0.234 kJ/mol. (c) Comparison of the MEPs of bcc Mg model (red circles) and bcc Mg with Nb's lattice parameter model (black squares).

Table 2. Energies of Mg/Nb slab configurations, relative to the energy of the bcc Mg/bcc Nb configuration relaxed along in-plane directions.

	Relaxation method	
Slab model	Relaxed along out-of-plane	Relaxed in all directions
bcc Mg/bcc Nb	0.000	0.001
pseudo-hcp Mg/bcc Nb	0.843	0.039

layer of 20 Å thickness was introduced to allow surface-like relaxation on the Mg film. Except for the constraint imposed by the Nb substrate, there are no additional strains or deformations imposed on the system. While the Nb atoms were constrained to relax only along the out-of-plane direction (experiments suggest that bcc Mg has lattice parameters corresponding to bcc Nb), two types of relaxations were considered for the Mg layers: relaxation along the direction perpendicular to the Mg/Nb interface and relaxation in all directions. As the results show, the bcc Mg/bcc Nb slab configuration with Mg relaxation constrained along in-plane directions is the most stable structure. The relative energies with respect to the energy of the most stable structure are presented in Table 2. When Mg atoms in the pseudo-hcp Mg/bcc Nb model are allowed to relax in all directions, they actually relax into a bcc-like configuration (with minor deviations due to surface relaxation effects). The slab calculations thus suggest that Mg layers prefer to align coherently to Nb bcc layers when the relative thickness of Mg is much smaller than that of Nb. This provides further validation to the analysis of the stability of bcc Mg in the bulk state and is in good agreement with the experimental observations. The structural variations calculated in the thin film models are presented in a supplement to the present article.

Conclusion In this paper, we have examined the stabilization of bcc Mg in Mg/Nb multilayer films [10] using calculations based on DFT. Under normal thermodynamic constraints, bcc Mg is unstable and this is manifested by the presence of an imaginary branch along the $\Gamma - N$ direction in the Brillouin zone, which is related in turn to the existence of a local maximum in the electronic DOS at the Fermi level. The observed stabilization of bcc Mg in Mg/Nb multilayer films is associated with the disappearance of the local maximum in the e-DOS at the Fermi level and results from the reduction in the lattice parameter of bcc Mg. Calculations of the Burgers transformation path between bcc and hcp show that bcc Mg with Nb's lattice parameter sits on a local minimum in the energy landscape when comparing bcc and hcp structures. This, along with the calculated hardening of the soft TA branch along the $\Gamma - N$ direction indicates that the stabilization of bcc Mg is mainly due to the mechanical constraints imposed when Mg is forced to (epitaxially) grow on bcc Nb. The stabilization of bcc Mg grown epitaxially on the bcc Nb substrate [10] is thus analogous to the stabilization of bcc Mg under high pressures.[7] Furthermore, the interface calculations show that Mg atoms prefer a bcc-like environment when they are in Mg/Nb thin films. These results provide further motivation to investigate the synthesis of Mg-based materials with properties not observed in bulk Mg by using thin film engineering. Based on this work, it is likely that similar stabilization effects can be generated by using other bcc substrates, as long as their lattice parameter is smaller than that of (fully relaxed) bcc Mg, the substrate is immiscible with Mg and is much stiffer than Mg. This stabilization can be further improved through the use of alloying, as demonstrated in the work by Tan et al.[6]

Supplementary online material A more detailed information on experiments is available at http://dx.doi.org/10.1080/21663831.2012.804218.

Acknowledgements Most of the calculations were carried out on the CAT cluster of the department of Chemical Engineering of Texas A&M University and the HYDRA and EOS clusters of Texas A&M Supercomputing facility. High-Performance Computing facilities from the Texas Advanced Computing Center in the University of Texas at Austin were also used. This research was supported by the National Science Foundation under NSF Grant No CBET-0932249 and partial support from the NSF Grant No. CMMI-0953984.

References

[1] Mordike BL, Ebert T. Magnesium: properties applications potential. Mater Sci Eng A. 2001;302(1):37–45.
[2] Taylor RH, Curtarolo S, Hart GLW. Ordered magnesium-lithium alloys: first-principles predictions. Phys Rev B. 2010;81(2):024112.
[3] Al-Samman T. Comparative study of the deformation behavior of hexagonal magnesiumlithium alloys and a conventional magnesium {AZ31} alloy. Acta Mater. 2009;57(7):2229–2242.
[4] Liu JZ, Zunger A. Thermodynamic states and phase diagrams for bulk-incoherent, bulk-coherent, and epitaxially-coherent semiconductor alloys: application to cubic (Ga,In)N. Phys Rev B. 2008;77(20):205201.
[5] Schapbach L, Züttel A. Hydrogen-storage materials for mobile applications. Nature. 2001;414:353–358.
[6] Tan X, Wang L, Holt CMB, Zahiri B, Eikerling MH, Mitlin D. Body centered cubic magnesium niobium hydride with facile room temperature absorption and four weight percent reversible capacity. Phys Chem Chem Phys. 2012;14:10904–10909.
[7] Olijnyk H, Holzapfel WB. High-pressure structural phase transition in Mg. Phys Rev B. 1985;31(7):4682–4683.
[8] Errandonea D, Boehler R, Ross M. Melting of the alkaline-earth metals to 80 GPa. Phys Rev B. 2001;65(1):012108.
[9] Errandonea D, Meng Y, Häusermann D, Uchida T. Study of the phase transformations and equation of state of

magnesium by synchrotron X-ray diffraction. J Phys-Condens Matter. 2003;15(8):1277–1289.
[10] Ham B, Zhang X. High strength Mg/Nb nanolayer composites. Mater Sci Eng A. 2011;528(4–5):2028–2033.
[11] Ham B, Junkaew A, Arróyave R, Chen J, Wang P, Majewski J, Park J, Zhou H-C, Arvapally R, Kaipa U, Omary MA, Zhang X, Ren Y, Zhang X. Hydrogen sorption in orthorhombic Mg hydride at ultralow temperature. Int J Hydrogen Energy. 2013, doi: http://dx.doi.org/10.1016/j.ijhydene.2013.04.098.
[12] Kresse G, Hafner J. *Ab initio* molecular dynamics for liquid metals. Phys Rev B. 1993;47(1):558–561.
[13] Kresse G, Joubert D. From ultrasoft pseudopotentials to the projector augmented-wave method. Phys Rev B. 1999;59(3):1758–1775.
[14] Wachowicz E, Kiejna A. Bulk and surface properties of hexagonal-close-packed Be and Mg. J Phys-Condens Matter. 2001;13(48):10767.
[15] Gurvich LV, Veyts IV, Alcock CB. Thermodynamic properties of individual substances. New York: Begell House; 1996.
[16] Hull AW. A new method of X-ray crystal analysis. Phys Rev. 1917;10(6):661–696.
[17] Wang Y, Curtarolo S, Jiang C, Arróyave R, Wang T, Ceder G, Chen L-Q, Liu Z-K. Ab initio lattice stability in comparison with CALPHAD lattice stability. Calphad. 2004;28(1):79–90.
[18] Smithells CJ, Gale WF, Totemeier TC. Smithells metals reference book. Amsterdam: Elsevier Butterworth-Heinemann; 2004.
[19] Dregia SA, Banerjee R, Fraser HL. Polymorphic phase stability in thin multilayers. Scripta Mater. 1998;39(2):217–223.
[20] Thompson GB, Banerjee R, Dregia SA, Fraser HL. Phase stability of bcc Zr in Nb/Zr thin film multilayers. Acta Mater. 2003;51(18):5285–5294.
[21] Mehta S, Price GD, Alfè D. Ab initio thermodynamics and phase diagram of solid magnesium: a comparison of the LDA and GGA. J Chem Phys. 2006;125(19):194507.
[22] Persson K, Ekman M, Ozoliņš V. Phonon instabilities in bcc Sc, Ti, La, and Hf. Phys Rev B. 2000;61(17):11221–11224.
[23] Luo W, Johansson B, Eriksson O, Arapan S, Souvatzis P, Katsnelson MI, Ahuja R. Dynamical stability of body center cubic iron at the earths core conditions. Proc Natl Acad Sci USA. 2010;107(22):9962–9964.
[24] Wang J, Li J, Yip S, Phillpot S, Wolf D. Mechanical instabilities of homogeneous crystals. Phys Rev B. 1995;52(17):12627–12635.
[25] Novaković N, Matović L, Novaković JG, Manasijević M, Ivanović N. Ab initio study of MgH2 formation. Mater Sci Eng B. 2009;165(3):235–238.
[26] Chen K, Boyle K. Elastic properties, thermal expansion coefficients, and electronic structures of Mg and Mg-based alloys. Metall Mater Trans A. 2009;40(11):2751–2760.
[27] Moriarty JA, McMahan AK. High-pressure structural phase transitions in Na, Mg, and Al. Phys Rev Lett. 1982;48(12):809–812.
[28] Burgers WG. On the process of transition of the cubic-body-centered modification into the hexagonal-close-packed modification of zirconium. Physica. 1934;1(7–12):561–586.
[29] Chen Y, Ho KM, Harmon BN. First-principles study of the pressure-induced bcc-hcp transition in Ba. Phys Rev B. 1988;37(1):283–288.
[30] Nishitani SR, Kawabe H, Aoki M. First-principles calculations on bcchcp transition of titanium. Mater Sci Eng A. 2001;312(1–2):77–83.
[31] Caspersen KJ, Lew A, Ortiz M, Carter EA. Importance of shear in the bcc-to-hcp transformation in iron. Phys Rev Lett. 2004;93(11):115501.
[32] Weinan E, Ren W, Vanden-Eijnden E. Simplified and improved string method for computing the minimum energy paths in barrier-crossing events. J Chem Phys. 2007;126(16):164103.
[33] E W, Ren W, Vanden-Eijnden E. String method for the study of rare events. Phys Rev B. 2002;66(5):052301.